Available online at www.sciencedirect.com

ScienceDirect

Procedia Computer Science 176 (2020) 3103–3111

Procedia Computer Science

www.elsevier.com/locate/procedia

24th International Conference on Knowledge-Based and Intelligent Information & Engineering Systems

Machine Learning and Data Fusion Techniques Applied to Physical Activity Classification Using Photoplethysmographic and Accelerometric Signals

Giorgio Biagetti[a], Paolo Crippa[a,*], Laura Falaschetti[a], Edoardo Focante[a], Natividad Martinez Madrid[b,d], Ralf Seepold[c,d], Claudio Turchetti[a]

[a]*DII — Department of Information Engineering, Università Politecnica delle Marche, via Brecce Bianche, 12, I-60131 Ancona, Italy*

[b]*Reutlingen University, Alteburgstr. 150, 72762 Reutlingen, Germany*

[c]*HTWG Konstanz, Alfred-Wachtel-Str. 8, 78462 Konstanz, Germany*

[d]*I.M. Sechenov First Moscow State Medical University, 2-4, Bolshaya Pirogovskaya st., 119435 Moscow, Russian Federation*

Abstract

The evaluation of the effectiveness of different machine learning algorithms on a publicly available database of signals derived from wearable devices is presented with the goal of optimizing human activity recognition and classification. Among the wide number of body signals we choose a couple of signals, namely photoplethysmographic (optically detected subcutaneous blood volume) and tri-axis acceleration signals that are easy to be simultaneously acquired using commercial widespread devices (e.g. smartwatches) as well as custom wearable wireless devices designed for sport, healthcare, or clinical purposes. To this end, two widely used algorithms (decision tree and k-nearest neighbor) were tested, and their performance were compared to two new recent algorithms (particle Bernstein and a Monte Carlo-based regression) both in terms of accuracy and processing time. A data preprocessing phase was also considered to improve the performance of the machine learning procedures, in order to reduce the problem size and a detailed analysis of the compression strategy and results is also presented.

Keywords: Machine learning; data fusion; activity classification; decision tree; kNN; photoplethysmography; PPG; acceleration

1. Introduction

Nowadays several research fields in computer science rely on machine learning algorithms for performing a large variety of tasks.

* Corresponding author. Tel.: +39-071-220-4541; fax: +39-071-220-4224.
E-mail address: p.crippa@univpm.it

1877-0509
10.1016/j.procs.2020.09.178

Recent advancements in wearable devices such as electrocardiography (ECG) [32, 25, 4], electroencephalography (EEG), surface electromyography (sEMG)[12, 11, 19], photoplethysmography (PPG)[2, 9, 36], and inertial data sensors have lead to a complex, large and heterogeneous data collection and processing [10, 17].

Manual investigation, analysis and processing of raw data coming from these sensors to obtain insightful information (e.g. physical activity being performed [6, 7] as well as diagnosis and prognosis of patients) is a difficult and time consuming task. Thus, implementing automatic knowledge-based decision-making systems is of paramount importance to exploit the large amount of data collected from these sensors. Due to their capability of performing the analysis of such complex data in a very efficient way, machine learning algorithms are playing a key role [27, 23] to identify data patterns and to give to the recognition systems the capability of learning from the identified data enabling more efficient and accurate decisions [24]. An example of decision-making system in healthcare is the recognition whether a hospital patient is suffering of a particular pathology or not [21, 3, 4, 25].

Photoplethysmography (PPG) is a noninvasive technique to monitor subcutaneous blood flow by measuring the light reflected by the skin. Unlike the ECG and the sEMG signals which need sticky metal electrodes across the skin to be acquired [10, 18], the PPG signal can be acquired at body peripheral sites and needs a simpler body contact. As a result, PPG sensors are becoming popular in wearable devices (smartwatches), as the preferred modality for heart rate monitoring in everyday activities. However, accurate estimation of PPG signal recorded from subject wrist, when the subject is performing various physical exercises, is often severely corrupted by motion artifacts (MAs) due to the relative movement between PPG light source/detector and the skin of the subject. In order to reduce the MAs, a number of signal processing techniques based on data derived from the smartphone built-in triaxial accelerometer have been proven to be very useful [14, 36, 9]. On the other hand, among wearable sensors, accelerometers are probably the most frequently used for activity monitoring[1, 26, 28, 13]. In particular, they are effective in monitoring actions that involve repetitive body motions, such as walking, running, cycling, climbing stairs [22, 31, 29, 33, 8].

Because the electrical signals collectable from patients are different and so heterogeneous, it is very important to perform experimental investigation to compare the performance of different machine learning algorithms to help select the ”winner” for a specific set of such signals.

A large number of machine learning algorithms have been developed in order to perform classification, regression, and in general pattern recognition. Among the most common algorithms we selected the decision tree (DT) [20] and the k-nearest neighbor (kNN) on the basis of their simple implementation and reduced computational time.

Among the wide number of body signals we choose a couple of signals PPG and tri-axis acceleration that are easy to be simultaneously acquired using commercial widespread devices (e.g. smartwatches) as well as custom wearable wireless devices designed for sport, healthcare, or clinical purposes.

We investigated their performance considering a dataset composed of both PPG and accelerometer signals in different conditions and compared their performance to those of two machine learning algorithms recently proposed, namely particle Bernstein polynomial (PBP) [16] and Monte Carlo-based regression (MCR) [34]. Accuracy and computational time have been compared in order to give a useful insight for designers in adopting the one that best fit the physical activity system they are implementing.

The rest of this paper is organized as follows: Section 2 is divided into two subsections that present the used data sets and machine learning algorithms, respectively. Section 3 discusses the experimental results and related findings. Finally, Section 4 gives some conclusions.

2. Material and Metods

2.1. Dataset

For testing and comparing the algorithms for human activity recognition from PPG and accelerometric signal we used a recent data set that is publicly available [15] Both the PPG and the accelerometer signals were simultaneously captured from the same wrist and are affected by motion artifacts. The dataset was recorded from seven subjects (three males and four females aged between 20 and 52 years) using the Maxim Integrated MAXREFDES100 device [1].

[1] https://www.maximintegrated.com/en/design/reference-design-center/system-board/6312.html

Participants performed five acquisition sessions each of squat exercises, stepper exercises, and resting. The dataset contains 210 recording sessions for a total duration of 17201 s and includes 105 PPG signals (15 for each subject) and the corresponding 105 triaxial accelerometer signals measured with a sampling frequency of 400 Hz.

2.2. Algorithms

To perform the classification task on the dataset, signals were first cut into possibly overlapping windows, where the window length and amount of overlapping had been subject to preliminary optimization as will be shown next.

Four classification algorithms were tested, decision tree, k-nearest neighbor, particle Bernstein polynomials, and Monte Carlo-based regression. Of these, the first two are natively classification algorithms, while the latter, more recently proposed, two, are natively regression algorithms that can be used for classification by applying them to an indicator function, defined as follows.

Assume that the input data x lies in a space Ω, that can subdivided into L disjoint subsets (classes) Ω_j, $j = 1, \ldots, L$, that cover the whole space $\Omega = \Omega_1 \cup \Omega_2 \cup \cdots \cup \Omega_L$. It is thus possible to define an indicator function

$$f(x) = \begin{cases} j & \text{if } x \in \Omega_j, \\ 0 & \text{otherwise} \end{cases} \tag{1}$$

that classifies each point $x \in \Omega$ to the corresponding class. It is of course the role of the classification algorithm to find appropriate boundaries for the various Ω_j, but this can be done by approximating the function (1) using known points from the training set and then rounding the result of the regression on an unknown sample to the nearest integer to determine its class.

2.2.1. Decision tree

This classifier partitions the input space into small segments, and labels these small segments with one of the various output categories. However, conventional decision tree only does the partitioning to the coordinate axes. With the growth of the tree, the input space can be partitioned into very small segments so as to recognize subtle patterns [30]. The main drawback is that overgrown trees could lead to overfitting.

2.2.2. K-nearest neighbor (kNN)

This classifier is one of the most popular neighborhood classifiers in pattern recognition and machine learning because of its simplicity and efficiency. It categorizes each unlabelled test example using the label of the majority of examples among its k-nearest (most similar) neighbors in the training data set. The similarity depends on a specific distance metric, therefore, the performance of the classifier strictly depends on the distance metric used. However, it suffers of memory requirements and time complexity, because it is fully dependent on every example in the training set [35].

2.2.3. Particle Bernstein polynomials

Bernstein polynomials have recently been proposed as an interesting basis for regression algorithms in machine learning contexts [5]. Bernstein polynomials of degree m in the interval $[0, 1]$ are defined as

$$b_k^m(x) = \binom{m}{k} x^k (1 - x)^{m-k}, \quad k = 0, 1, \ldots, m \tag{2}$$

where $\binom{m}{k}$ denotes the binomial coefficient. They have the property that, given a function $f(x)$ in $[0, 1]$, their linear combination, with coefficients equal to the function evaluated on a uniform grid, converges uniformly to f as m

increases, i.e.

$$\lim_{m\to\infty} \sum_{k=0}^{m} f\left(\frac{k}{m}\right) b_k^m(x) = f(x)\,. \tag{3}$$

This approach does not require any computation, besides the target function evaluation, to determine the coefficients, and can straightforwardly be extended to multidimensional inputs. But the requirement of the uniform grid soon becomes impractical as the dimensionality d of the input space increases.

To avoid this shortcoming Particle-Bernstein Polynomials (PBPs) had also recently been proposed, which no longer depend on a uniform sampling of the target function. They are defined as

$$C_\xi^m(x) = \alpha_\xi^m\, x^\xi\, (1-x)^{m-\xi} = \alpha_\xi^m\, k_\xi^m(x) \tag{4}$$

where ξ is a *real* number such that $0 \le \xi \le m$, thus removing the constraint of integral grid subdivisions, and α_ξ^m are normalization factors that ensure the basis function have unitary area

$$\int_0^1 C_\xi^m(x)\,dx = 1\,. \tag{5}$$

PBPs functions have a maximum at $x = \xi/m$, and for $m \gg 1$ may be used to approximately "sample" the target function at an arbitrary point $0 \le \xi/m \le 1$

$$f(\xi/m) \simeq \int_0^1 f(x)\, C_\xi^m(x)\,dx\,. \tag{6}$$

If the value of target function is known at points $x^{(j)}$ from some experimental data, the integral in (6) can be approximated by a discrete summation over j, and taking into account the normalization factors from (5), it results

$$f(\xi/m) \simeq \frac{\sum_{j=1}^N f(x^{(j)}) k_\xi^m(x^{(j)})}{\sum_{j=1}^N k_\xi^m(x^{(j)})} \tag{7}$$

that also holds in case of multivariate data.

2.2.4. Monte Carlo-based regression

This method can be viewed as a generalization of (7) to different basis functions. It lays its roots on kernel-based function approximation (see [34] for a formal derivation), so that, if k_m is a kernel function, with m sufficiently large, we can approximate the target function as

$$f(x) \simeq \frac{\sum_{j=1}^N f(x^{(j)})\, k_m(x - x^{(j)})}{\sum_{j=1}^N k_m\,(x - x^{(j)})}\,. \tag{8}$$

Often a Gaussian kernel is used, $k_m(x) = \exp\left(-\frac{1}{2}m^2\|x\|^2\right)$, so that (8) becomes

$$f(x) \simeq \frac{\sum_{j=1}^{N} f(x^{(j)}) \exp\left(-\frac{1}{2}m^2\|x - x^{(j)}\|^2\right)}{\sum_{j=1}^{N} \exp\left(-\frac{1}{2}m^2\|x - x^{(j)}\|^2\right)} . \tag{9}$$

3. Experimental Results

A first experiment was performed to identify the best window length with whom to segment the raw signals. The "traditional" DT and kNN classifiers were used for this task. Of the seven subjects available in the dataset used for experimentation, five were used to train the different classifiers, and the last two subjects were reserved for the evaluation of the accuracy. Table 1 shows the accuracy of the classifiers using, respectively, PPG data alone, accelerometer (ACC) data alone, and a feature vector composed of PPG and ACC data concatenated together to perform a data fusion between the two sensors.

Table 1. Classification accuracy of the "traditional" classifiers for different window lengths.

	PPG		ACC		Data Fusion	
Window	DT	kNN	DT	kNN	DT	kNN
1000	60.87%	65.72%	83.80%	81.03%	**88.40%**	**79.33%**
1100	**66.67%**	65.83%	71.11%	**84.10%**	71.46%	78.26%
1200	58.73%	65.80%	71.05%	81.92%	71.73%	76.52%
1300	63.21%	65.02%	71.77%	83.62%	71.76%	77.44%
1400	64.35%	**68.00%**	**84.44%**	82.40%	85.06%	77.95%
1500	62.55%	65.97%	83.36%	83.27%	87.74%	78.04%
1600	59.95%	66.36%	84.05%	81.50%	87.70%	77.85%
1700	58.25%	66.45%	83.06%	81.88%	87.05%	78.75%
1800	57.27%	66.09%	70.10%	81.44%	70.10%	77.89%
1900	65.86%	66.71%	83.17%	81.96%	83.65%	77.24%
2000	58.78%	67.05%	78.63%	81.42%	78.88%	79.00%

Window lengths and overlaps are expressed as number of signal samples, with the sample rate being 400 Hz, so as to explore the range between 2.5 s and 5.0 s, which are reasonable time spans to execute a single exercise of the types included (squat and step) in the dataset. As can be seen, the data fusion approach somehow outperforms the single-signal approach when using DT, while kNN probably suffers from the increased dimensionality.

To gain further insights, the fused data was tested with overlapped windows. Table 2 and 3 report the classification accuracies for the DT and kNN algorithms, respectively, for all the considered window lengths and with varying degree of overlap, from zero (i.e., the previous experiment) to 600 samples.

Table 2. Classification accuracy vs. window length (rows) and overlap (columns), using the DT classifier.

Window	0	100	200	300	400	500	600
1000	88.40%	84.81%	89.42%	77.27%	78.89%	**90.27%**	89.61%
1100	71.46%	88.57%	84.87%	89.25%	76.74%	79.32%	90.16%
1200	71.73%	71.35%	88.29%	71.69%	88.84%	77.11%	78.97%
1300	71.76%	71.74%	70.76%	88.27%	85.36%	88.85%	76.45%
1400	85.06%	71.99%	76.13%	70.58%	88.79%	86.17%	89.55%
1500	87.74%	85.12%	72.11%	75.38%	75.46%	88.58%	85.53%
1600	87.70%	85.63%	86.16%	72.81%	75.38%	76.00%	88.88%
1700	87.05%	83.01%	82.92%	85.79%	72.78%	74.20%	75.77%
1800	70.10%	87.14%	82.36%	82.97%	84.63%	73.23%	74.23%
1900	83.65%	70.38%	85.06%	83.38%	87.91%	85.25%	76.69%
2000	78.88%	83.41%	70.38%	85.27%	82.36%	87.72%	85.41%

Table 3. Classification accuracy vs. window length (rows) and overlap (columns), using the kNN classifier.

Window	0	100	200	300	400	500	600
1000	79.33%	79.41%	78.43%	78.42%	78.81%	79.24%	78.91%
1100	78.26%	79.29%	**79.58%**	78.46%	78.52%	78.56%	79.23%
1200	76.52%	78.23%	78.92%	79.22%	78.54%	78.13%	78.63%
1300	77.44%	77.53%	78.16%	78.69%	78.79%	79.02%	77.87%
1400	77.95%	77.18%	77.42%	77.57%	78.28%	78.26%	78.74%
1500	78.04%	77.63%	76.90%	77.22%	77.07%	77.93%	78.29%
1600	77.85%	77.93%	77.32%	76.86%	76.99%	77.05%	77.83%
1700	78.75%	77.62%	77.77%	77.30%	77.43%	77.11%	76.97%
1800	77.89%	78.92%	77.47%	77.13%	77.12%	77.47%	76.99%
1900	77.24%	77.73%	78.79%	77.68%	77.26%	76.85%	77.60%
2000	79.00%	77.24%	77.84%	78.87%	77.68%	77.45%	76.81%

As can be seen, shorter windows tend to behave better than the longer ones.

Focusing the attention on the two best cases so far obtained, a dimensionality reduction by means of a PCA was performed. The optimal number of retained components was searched by performing experiments using a window length of 1000 with 50% overlap (Table 4) and using a window length of 1100 with 200 samples of overlap (Table 5), being the two best candidates obtained so far.

Table 4. Classification accuracy after dimensionality reduction by PCA. 1000 samples windows with 500 samples overlap case.

PCA Components	kNN	DT
5	73.28%	73.79%
10	84.85%	75.12%
15	86.09%	74.42%
20	88.43%	74.52%
25	89.92%	74.23%
30	**93.88%**	74.29%
35	93.66%	74.29%
40	92.71%	74.29%

Table 5. Classification accuracy after dimensionality reduction by PCA. 1100 samples windows with 200 samples overlap case.

PCA Components	kNN	DT
5	74.63%	77.08%
10	89.08%	77.36%
15	93.69%	77.36%
20	**94.20%**	77.36%
25	93.57%	77.36%
30	92.83%	77.36%
35	92.66%	77.36%
40	92.32%	77.36%

As can clearly be seen, PCA reverses the odds in favour of kNN, which exhibit much higher accuracies except for the first row which employed a very small number of retained components.

Finally, once the optimal number of components had been found, the two newer algorithms were tested on them. Since these two algorithms are regression-based, the following mapping of the classes was used: 1 – rest, 2 – squat, 3 – step. Results, including computation time, can be seen in Tables 6 and 7.

Table 6. Final results with a 1000/500 windowing, 30 components, PBP order 35, MCR order 10.

	kNN	PBP	MCR
Accuracy	93.88%	96.23%	94.90%
Training Time	0.753 s	0	0
Testing Time	0.298 s	250.152 s	7.289 s

Table 7. Final results with a 1100/200 windowing, 20 components, PBP order 40, MCR order 10.

	kNN	PBP	MCR
Accuracy	94.20%	96.42%	96.08%
Training Time	0.046 s	0	0
Testing Time	0.054 s	51.086 s	1.992 s

In both cases, the newer classification methods performed better than kNN, though at the cost of a somewhat higher computation time.

The confusion matrices corresponding to these tables are reported in Fig. 1 and 2, respectively.

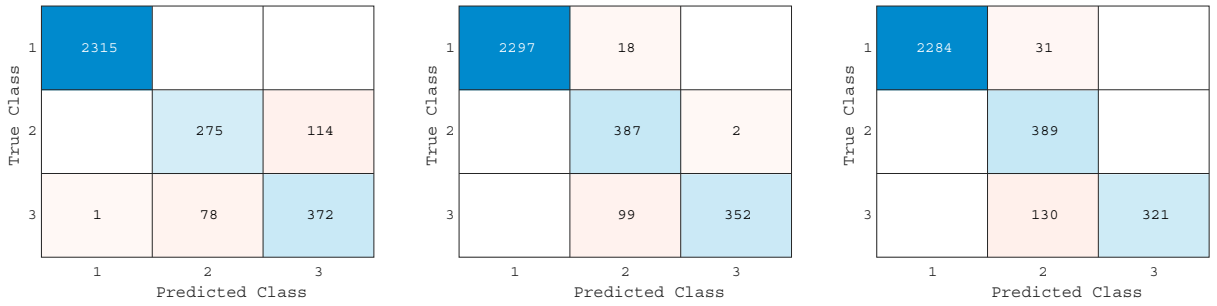

Fig. 1. Confusion matrices with a 1000/500 windowing, for kNN, PBP order 35 and MCR order 10, respectively.

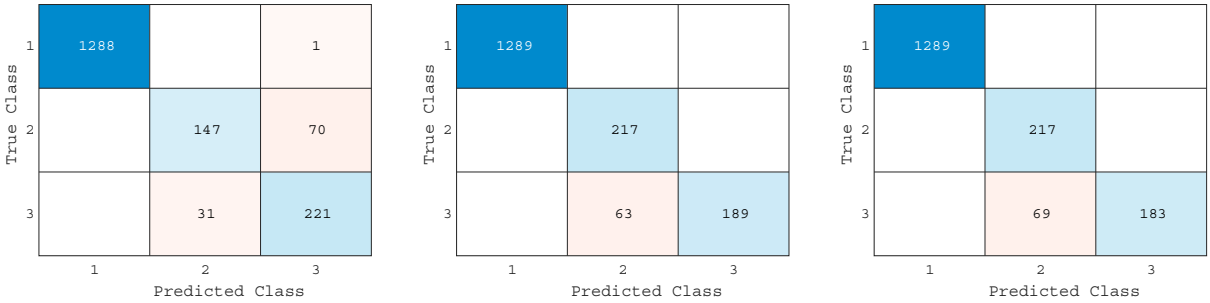

Fig. 2. Confusion matrices with a 1100/200 windowing, for kNN, PBP order 35 and MCR order 10, respectively.

From these, it is possible to see that the newer algorithms (PBP and MCR) did a better job at resolving class 2, especially in the 1100/200 case.

4. Conclusions

In this paper we investigated the performance of a few different classification algorithms applied to the recognition of three different human activities, based on the recording of inertial signals and PPG signals derived from a publicly available dataset. Amongst the tested traditional algorithms kNN resulted the most efficient, and so it was compared with two newer algorithms to give some insights as to which system performs best in this type of recognition problems. The newer algorithms proved to be able to achieve better overall accuracy, though at the expense of a somewhat higher computation time.

Acknowledgements

This research was partially supported by a Università Politecnica delle Marche Research Grant.

References

[1] Anguita, D., Ghio, A., Oneto, L., Parra, X., Reyes-Ortiz, J.L., 2013. Energy efficient smartphone-based activity recognition using fixed-point arithmetic. Journal of Universal Computer Science 19, 1295–1314.

[2] Bacà, A., Biagetti, G., Camilletti, M., Crippa, P., Falaschetti, L., Orcioni, S., Rossini, L., Tonelli, D., Turchetti, C., 2015. CARMA: A robust motion artifact reduction algorithm for heart rate monitoring from PPG signals, in: 23rd European Signal Processing Conference (EUSIPCO 2015), Nice, France. pp. 2696–2700.

[3] Begum, S., Ahmed, M.U., Funk, P., Xiong, N., Folke, M., 2011. Case-based reasoning systems in the health sciences: A survey of recent trends and developments. IEEE Transactions on Systems, Man, and Cybernetics, Part C (Applications and Reviews) 41, 421–434.

[4] Biagetti, G., Crippa, P., Curzi, A., Orcioni, S., Turchetti, C., 2014. A multi-class ECG beat classifier based on the truncated KLT representation, in: 2014 European Modelling Symposium, Pisa, Italy. pp. 93–98.

[5] Biagetti, G., Crippa, P., Falaschetti, L., Luzzi, S., Santarelli, R., Turchetti, C., 2019a. Classification of Alzheimer's disease from structural magnetic resonance imaging using particle-Bernstein polynomials algorithm, in: Czarnowski, I., Howlett, R.J., Jain, L.C. (Eds.), Intelligent Decision Technologies 2019, Springer Singapore, Singapore. pp. 49–62.

[6] Biagetti, G., Crippa, P., Falaschetti, L., Luzzi, S., Turchetti, C., 2019b. Recognition of daily human activities using accelerometer and sEMG signals, in: Czarnowski, I., Howlett, R.J., Jain, L.C. (Eds.), Intelligent Decision Technologies 2019, Springer Singapore, Singapore. pp. 37–47.

[7] Biagetti, G., Crippa, P., Falaschetti, L., Orcioni, S., Turchetti, C., 2015. A rule based framework for smart training using sEMG signal, in: Neves-Silva, R., Jain, L.C., Howlett, R.J. (Eds.), Intelligent Decision Technologies. Springer International Publishing. volume 39 of *Smart Innovation, Systems and Technologies*, pp. 89–99.

[8] Biagetti, G., Crippa, P., Falaschetti, L., Orcioni, S., Turchetti, C., 2016a. An efficient technique for real-time human activity classification using accelerometer data, in: Intelligent Decision Technologies 2016: Proceedings of the 8th KES International Conference on Intelligent Decision Technologies – Part I. Springer International Publishing, Cham, Switzerland, pp. 425–434.

[9] Biagetti, G., Crippa, P., Falaschetti, L., Orcioni, S., Turchetti, C., 2016b. Motion artifact reduction in photoplethysmography using Bayesian classification for physical exercise identification, in: Proceedings of the 5th International Conference on Pattern Recognition Applications and Methods (ICPRAM 2016), Rome, Italy. pp. 467–474.

[10] Biagetti, G., Crippa, P., Falaschetti, L., Orcioni, S., Turchetti, C., 2016c. Wireless surface electromyograph and electrocardiograph system on 802.15.4. IEEE Transactions on Consumer Electronics 62, 258–266.
[11] Biagetti, G., Crippa, P., Falaschetti, L., Orcioni, S., Turchetti, C., 2017. Homomorphic deconvolution for MUAP estimation from surface EMG signals. IEEE Journal of Biomedical and Health Informatics 21, 328–338.
[12] Biagetti, G., Crippa, P., Falaschetti, L., Orcioni, S., Turchetti, C., 2018a. Human activity monitoring system based on wearable sEMG and accelerometer wireless sensor nodes. BioMedical Engineering Online 17.
[13] Biagetti, G., Crippa, P., Falaschetti, L., Orcioni, S., Turchetti, C., 2018b. Human activity recognition using accelerometer and photoplethysmographic signals, in: Czarnowski, I., Howlett, R.J., Jain, L.C. (Eds.), Intelligent Decision Technologies 2017, Springer International Publishing, Cham, Switzerland. pp. 53–62.
[14] Biagetti, G., Crippa, P., Falaschetti, L., Orcioni, S., Turchetti, C., 2019c. Reduced complexity algorithm for heart rate monitoring from PPG signals using automatic activity intensity classifier. Biomedical Signal Processing and Control 52, 293–301.
[15] Biagetti, G., Crippa, P., Falaschetti, L., Saraceni, L., Tiranti, A., Turchetti, C., 2020a. Dataset from PPG wireless sensor for activity monitoring. Data in Brief 29.
[16] Biagetti, G., Crippa, P., Falaschetti, L., Turchetti, C., 2017. Machine learning regression based on particle Bernstein polynomials for nonlinear system identification, in: 2017 IEEE 27th International Workshop on Machine Learning for Signal Processing (MLSP), Tokyo, Japan. pp. 1–6.
[17] Biagetti, G., Crippa, P., Falaschetti, L., Turchetti, C., 2020b. A multi-channel electromyography, electrocardiography and inertial wireless sensor module using Bluetooth low-energy. Electronics 9.
[18] Biagetti, G., Crippa, P., Orcioni, S., Turchetti, C., 2016d. An analog front-end for combined EMG/ECG wireless sensors, in: Mobile Networks for Biometric Data Analysis. Springer International Publishing, Cham, Switzerland, pp. 215–224.
[19] Biagetti, G., Crippa, P., Orcioni, S., Turchetti, C., 2016e. Surface EMG fatigue analysis by means of homomorphic deconvolution, in: Mobile Networks for Biometric Data Analysis. Springer International Publishing, Cham, Switzerland, pp. 173–188.
[20] Breiman, L., Friedman, J., Olshen, R., Stone, C., 1984. Classification and Regression Trees. Wadsworth & BrooksCole Advanced Books & Software, Monterey, CA.
[21] Caruana, R., Niculescu-Mizil, A., 2006. An empirical comparison of supervised learning algorithms, in: Proceedings of the 23rd International Conference on Machine Learning, Association for Computing Machinery, New York, NY, USA. pp. 161–168.
[22] Catal, C., Tufekci, S., Pirmit, E., Kocabag, G., 2015. On the use of ensemble of classifiers for accelerometer-based activity recognition. Applied Soft Computing 37, 1018–1022.
[23] Christopher, M.B., 2016. Patter Recognition and Machine Learning. Springer-Verlag New York.
[24] Clifton, D.A., Gibbons, J., Davies, J., Tarassenko, L., 2012. Machine learning and software engineering in health informatics, in: 2012 First International Workshop on Realizing AI Synergies in Software Engineering (RAISE), Zurich, Switzerland. pp. 37–41.
[25] Crippa, P., Curzi, A., Falaschetti, L., Turchetti, C., 2015. Multi-class ECG beat classification based on a Gaussian mixture model of Karhunen-Loève transform. International Journal of Simulation – Systems, Science & Technology 16, 2.1–2.10.
[26] Dernbach, S., Das, B., Krishnan, N.C., Thomas, B.L., Cook, D.J., 2012. Simple and complex activity recognition through smart phones, in: 8th International Conference on Intelligent Environments, Guanajuato, Mexico. pp. 214–221.
[27] Duda, R.O., Hart, P.E., Stork, D.G., 2012. Pattern classification. John Wiley & Sons.
[28] Khan, A.M., Lee, Y.K., Lee, S., Kim, T.S., 2010. Human activity recognition via an accelerometer-enabled-smartphone using kernel discriminant analysis, in: 2010 5th International Conference on Future Information Technology, Busan, South Korea. pp. 1–6.
[29] Mannini, A., Intille, S.S., Rosenberger, M., Sabatini, A.M., Haskell, W., 2013. Activity recognition using a single accelerometer placed at the wrist or ankle. Medicine and Science in Sports and Exercise 45, 2193–2203.
[30] Quinlan, J.R., 1986. Induction of decision trees. Machine Learning 1, 81–106.
[31] Rodriguez-Martin, D., Samà, A., Perez-Lopez, C., Català, A., Cabestany, J., Rodriguez-Molinero, A., 2013. SVM-based posture identification with a single waist-located triaxial accelerometer. Expert Systems with Applications 40, 7203–7211.
[32] Scherz, W.D., Seepold, R., Martínez Madrid, N., Crippa, P., Biagetti, G., Falaschetti, L., Turchetti, C., 2019. Activity monitoring and phase detection using a portable EMG/ECG system, in: Saponara, S., De Gloria, A. (Eds.), Applications in Electronics Pervading Industry, Environment and Society, Springer International Publishing, Cham, Switzerland. pp. 187–194.
[33] Torres-Huitzil, C., Nuno-Maganda, M., 2015. Robust smartphone-based human activity recognition using a tri-axial accelerometer, in: 2015 IEEE 6th Latin American Symposium on Circuits Systems (LASCAS), Montevideo, Uruguay. pp. 1–4.
[34] Turchetti, C., Falaschetti, L., 2018. A GPU parallel algorithm for non parametric tensor learning, in: 2018 IEEE International Symposium on Signal Processing and Information Technology (ISSPIT), Louisville, KY, USA. pp. 286–290.
[35] Weinberger, K.Q., Saul, L.K., 2009. Distance metric learning for large margin nearest neighbor classification. Journal of Machine Learning Research 10, 207–244.
[36] Zhang, Z., Pi, Z., Liu, B., 2015. TROIKA: A general framework for heart rate monitoring using wrist-type photoplethysmographic signals during intensive physical exercise. IEEE Transactions on Biomedical Engineering 62, 522–531.